

BRIEF COMMUNICATION OPEN



Electrode array probe designed for visualising and monitoring multiple localised corrosion processes and mechanisms simultaneously occurring on marine structures

Majid Laleh^{1,2}, Ying Huo^{1,2}, Robert E. Melchers³ and Mike Yongjun Tan^{1,2}✉

An electrode array probe has been specially designed and demonstrated for in situ monitoring and visualising multiple localised corrosion processes and mechanisms, including crevice, weldment and pitting corrosion, occurring simultaneously on marine steel structures. It enabled the probing of time-dependent development of multiple localised corrosion processes, mechanisms and kinetics, thereby facilitating more in-depth understanding of the initiation, propagation and kinetics of localised corrosion of steel marine structures.

npj Materials Degradation (2023)7:68; <https://doi.org/10.1038/s41529-023-00388-9>

Marine corrosion and its prevention have been explored extensively by many scientists and engineers over the past two centuries¹. Over the recent decades, significant effort has been made to achieve a clearer understanding of marine corrosion mechanisms and factors affecting corrosion behaviour and kinetics in the ocean^{2,3} and to develop corrosion models for predicting marine corrosion for steel structures^{4,5}. This includes the so-called 'bi-modal' corrosion model that shows marine corrosion following a non-linear trend for an early time period (namely Mode 1), followed by another much longer trend (namely Mode 2)^{2,3,6–11}. The bi-modal behaviour has been explained based on the classical corrosion theory^{1,12,13} and more recent experimental evidence^{2,3,6–11,14,15}. However, more direct experimental observation of the corrosion mechanisms involved, particularly for localised corrosion, is still needed because the conventional methods of acquiring marine corrosion data largely rely on the use of metal coupons for mass loss estimates and for pit depth data^{6,7}. Particularly in view of recent experimental evidence for the influence of pitting in the overall development of the corrosion process, it can be argued that these traditional methods have limited temporal and/or spatial resolution to visualise the changing localised corrosion processes and mechanisms such as crevice corrosion, weldment corrosion and under-deposit corrosion¹⁶ that are known to be subject to environmental variabilities¹⁷. This Brief Communication reports an electrode array probe that is shown to be able to simulate and visualise multiple forms of localised marine corrosion of steel with in situ and site-specific capabilities for corrosion data acquisition. Although various electrode array probes have been reported previously for localised corrosion studies^{18–20}, the probe described below has the capability of simulating, visualising and monitoring the co-existence of multiple types of localised corrosion that commonly occur on marine steel structures such as offshore steel pipelines.

PROBE DESIGNED FOR MONITORING MULTIPLE LOCALISED CORROSION

Offshore pipelines are known to be prone to pitting and crevice corrosion at welds along and between segments of pipes and crevice corrosion at bolts (heads, butts, washers) on flanges

between spools and between flanges bolted together. As shown in Figs. 1c1 and 2, a specially designed electrode array probe was made by electrochemically integrating 100 electrodes that were cut out of a strip of pipeline with a weldment zone. A three-dimensional electrode structure was added to the electrode array surface to simulate a crevice zone. In this way, several localised corrosion conditions are simulated on a single electrode array probe. More details on the probe design and experimental are described in the 'Method' section below.

IN SITU MONITORING OF CORROSION PROCESSES IN THE OCEAN

The capabilities of the electrode array corrosion probe were demonstrated by the in situ electrochemical monitoring of the initiation and propagation of localised forms of metal corrosion over 61 weeks of exposure in actual ocean conditions. Figure 1a, b show corrosion data obtained from field testing using the probe designed to simulate an offshore pipeline that has both crevices and weldments on it. Figure 1a shows that at the very beginning of the exposure of the probe to ocean seawater, corrosion initiation started within the crevice area, as indicated by the reddish colour in the maps. In order to simulate and evaluate the effect of cathodic protection on marine structures, a cathodic protection potential of -900mV vs Cu/CuSO₄ reference electrode was applied to the probe for a short period of time (approximately 2 hours). Under cathodic potential, corrosion in the crevice area reduced to almost zero with all the electrodes in the electrode array showing negative cathodic or zero currents, as indicated by bluish and white colours in Fig. 1a. It can be seen in Fig. 1a that when cathodic protection was applied on the electrode array surface, cathodic currents, as indicated by the bluish colours, penetrated to the top part of the crevice area (close to the crevice mouth), suggesting that cathodic protection worked in this part of the crevice area. The bottom part of the crevice, however, registered almost zero current, as indicated by the white colour, suggesting no cathodic protection current in this area. This is reasonable since it is well-known that cathodic currents cannot travel a long distance within a narrow crevice. The bottom part of the crevice was protected from corrosion because cathodic

¹School of Engineering, Deakin University, Waurn Ponds, VIC 3216, Australia. ²Institute for Frontier Materials, Deakin University, Waurn Ponds, VIC 3216, Australia. ³Centre for Infrastructure Performance and Reliability, University of Newcastle, University Drive, Callaghan, NSW 2308, Australia. ✉email: mike.tan@deakin.edu.au

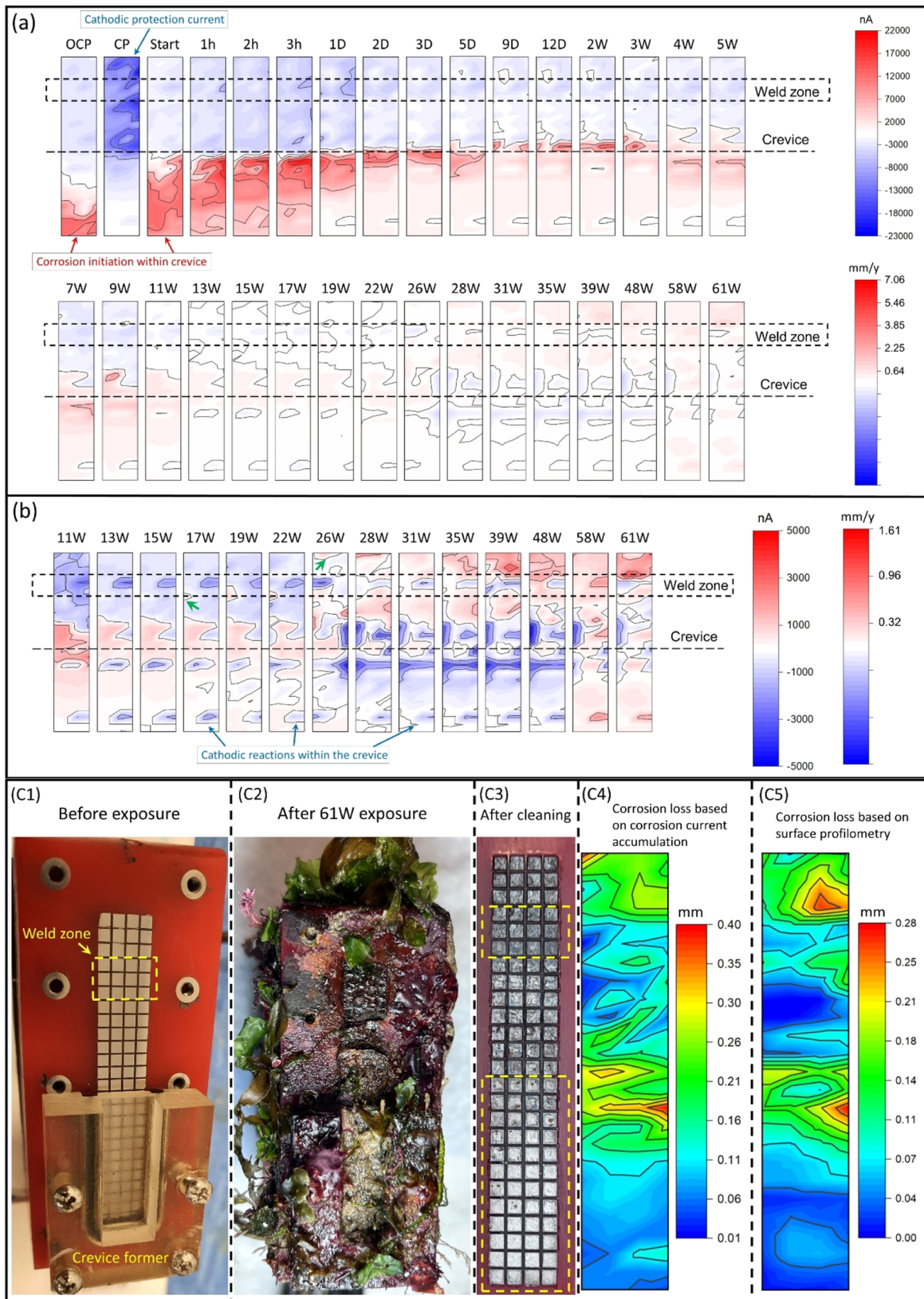


Fig. 1 In situ monitoring of corrosion processes in the ocean. **a** Current maps measured from the electrode array surface after different periods of exposure in the Queenscliff Ocean, Victoria, Australia. **b** Magnified current maps for the period range of week 11 to week 61. Green arrows in **b** indicate the locations where the localised corrosion in HAZ was active. Photo of the probe (**c1**) before and (**c2**) after 61 W exposure to seawater, and (**c3**) after cleaning the probe according to ASTM standard G1-03. Calculated corrosion loss: (**c4**) based on the corrosion current accumulation and (**c5**) based on the weight loss measurements from surface profilometry.

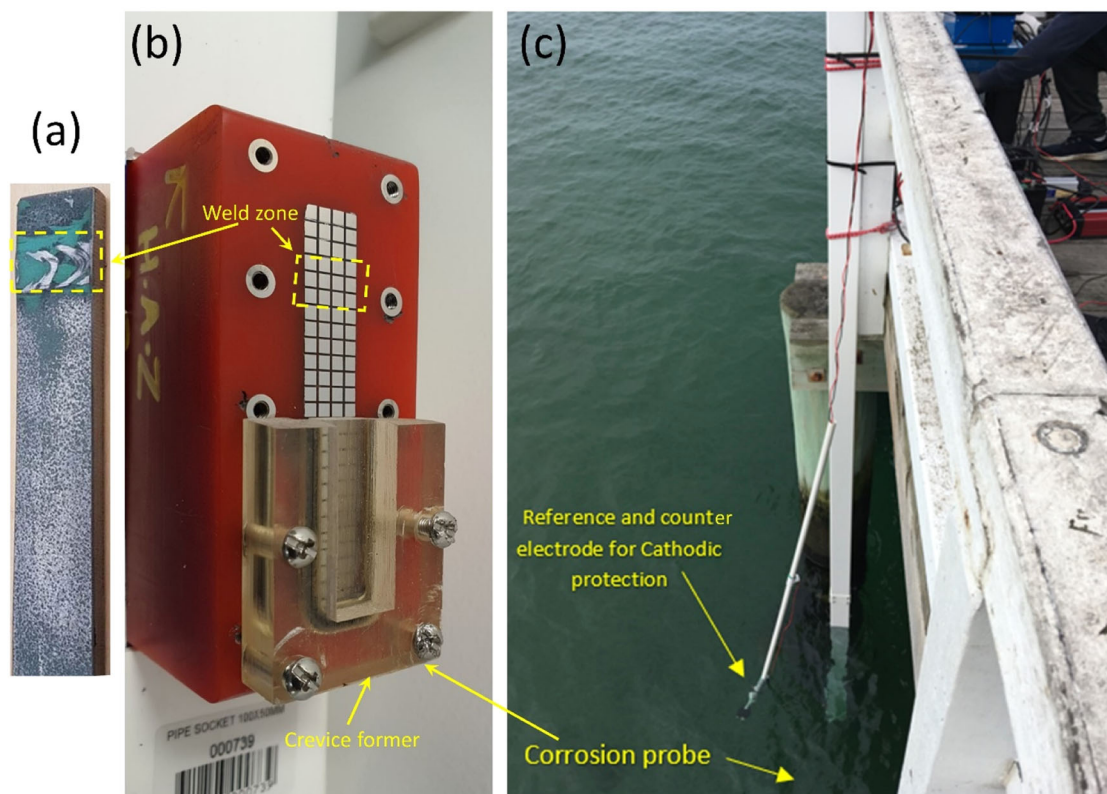


Fig. 2 Corrosion probe field testing. Probe design and field testing setup. **a** A rectangle section of API X65 pipeline with the weld zone sitting at one end marked by a dashed rectangle. **b** Photographs of the designed electrode array probe to simulate the co-existence of crevice corrosion and pitting/weldment corrosion at welds. **c** Field testing at Queenscliff Ocean site.

reactions consumed all oxidants such as oxygen in this enclosed crevice area and therefore no corrosion reaction existed there. After the cathodic protection was switched off, active corrosion recommenced inside the crevice and reached up to 7 mm/y within about half an hour. Within a few days, the crevice corrosion moved outwards, that is, towards the crevice mouth. Most corrosion initiated and propagated around the crevice and its mouth areas, as shown in enlarged maps in Fig. 1b. These observations are in agreement with industry experience that the greatest degree of crevice corrosion tends to occur at locations such as on flanges between spools, between flanges bolted together, and at end plates on parked pipelines in the ocean.

Careful observation of the corrosion maps in Fig. 1b shows that from week 17 onwards the active corrosion zone moved gradually toward the weldment areas (see green arrows). For the welds, the corrosion sites are close to the heat-affected zone (HAZ) on one side of the weld zone, suggesting that the HAZ acted as an anode, with the rest of the weldment acting as the cathode. After about 26 weeks of exposure, major localised corrosion started to occur at the HAZ zones on both sides of the weld. Galvanic corrosion between different zones likely contributed to this behaviour because the weld metal, base metal and the HAZ are known to differ both in composition and microstructures. Overall these results are in general agreement with those from marine immersion exposures of welds on steel coupons in temperate seawater^{8,9} and complement observations for some longer-term exposure (up to 16 years) experiments^{21–25}. The results in Fig. 1a, b show the development with time of the dynamics for the corrosion processes at crevices and welds. Figure 1c2 shows the probe surface after 61 weeks of seawater exposure. The probe surface shown in Figure 1c3 (after removing corrosion products) appears in good agreement with the map of weight losses calculated based on the accumulated corrosion currents, as shown

in Fig. 1c4, as well as the map of weight losses measured from surface profilometry, as shown in Fig. 1c5. The patterns of corrosion losses calculated based on accumulated corrosion currents and based on surface profilometry, as shown in Fig. 1c4, c5, are similar although the maximum corrosion losses have some differences (0.40 mm vs. 0.28 mm). Such differences could be due to several possible reasons: (i) only a limited number of corrosion current maps shown in Fig. 1a were used to calculate the accumulated corrosion map; and (ii) the galvanic currents measured by the probe do not contain 'uniform corrosion' currents in each individual electrodes, which have already been discussed in earlier publications¹⁹; (iii) surface profilometry can also have measurement errors. Overall, the initiation and propagation processes of multiple localised corrosion occurring simultaneously on the probe surface are revealed.

ANALYSIS OF LOCALISED CORROSION MECHANISMS

As shown in Fig. 1c2, the corrosion probe was covered with corrosion products and marine growth, especially at the crevice area. Observations using an underwater camera showed that after some 35 weeks of exposure the probe surface especially the crevice area was covered by corrosion products and marine growth. This suggests that after extended exposure to seawater, the corrosion cells inside the crevice should be separated from those outside the crevice and that inward diffusion of oxygen should become increasingly difficult. Oxygen concentration within the crevice would be reduced and depleted, and therefore oxygen reduction would cease to be the governing cathodic reaction within the crevice area. However, as shown in Fig. 1b, the cathodic reaction did not cease within the crevice itself. This suggests that there must be a different cathodic reaction, other than oxygen reduction, occurring within the crevice. The most probable

explanation is that the hydrolysis of ferrous and ferric ions (from the corrosion reaction) produced hydrogen ions (H^+), leading to a reduction in local pH (acidification) within the crevice area. Corrosion would thus occur within the crevice with hydrogen evolution reaction as the 'new' cathodic reaction. This is in agreement with a theory proposed earlier^{8,9} and provides direct evidence for explaining the bi-modal model behaviour. In Mode 1 of the bi-modal model, the governing cathodic reaction for corrosion is the consumption of oxygen, which can be considered an 'aerobic' process, governed by the rate of the cathodic oxygen reduction reaction⁹. Subsequently, as access by oxygen becomes increasingly difficult because of the build-up of corrosion products and marine growth, Mode 2 takes over. In Mode 2 oxygen is not required for the corrosion reactions because corrosion occurs largely under anaerobic conditions⁹, specifically the hydrogen evolution reaction⁹. These results demonstrate that the electrode array probe enabled the in situ electrochemical monitoring and understanding of complex and multiple localised corrosion processes and mechanisms.

METHODS

The electrode array probe used in this study, as shown in Fig. 2, consists of 100 square electrodes of the same dimension (2.3×2.3 mm) with the gap between the adjacent electrodes being 0.27 mm, which is arranged in 25 by 4 array creating a rectangle with a surface area of 64 mm by 10 mm. This electrode array pattern was produced on the steel strip including a weldment zone (Fig. 2a) using wire cutting, and the cut pieces were carefully re-assembled to make sure that the pieces were in the same spot as in the original steel strip and were firmly held in place and isolated from each other by epoxy. To simulate the crevice area that could exist on offshore pipelines (e.g., under disbanded coatings, on flanges between pipe spools, between flanges bolted together, and at end plates on parked pipelines), the electrode array was partially covered with a 0.9 mm thick polymethyl methacrylate cover (as crevice former) with the crevice gap size set as 1 mm. Twelve rows of electrode array were covered by crevice former while thirteen rows (including the weld zone) were kept outside the crevice directly in contact with the environment. Prior to the exposure, the array surface was abraded with SiC papers down to 1200 grit finish using water as a lubricant and then rinsed with ethanol.

Field tests were performed by exposing the corrosion probe to natural ocean seawater at Queenscliff, Victoria, Australia. Prior to immersion into the ocean, the crevice was carefully filled with seawater to avoid trapping air in the crevice area. Figure 2c illustrates the test location and the test setup. The depth of water in that area was almost 4 metres. At the test location, the corrosion probe was attached to a pile of the Queenscliff pier. Data collection was carried out regularly; daily measurements during the first two weeks of exposure in order to capture the corrosion initiation stages. Thereafter the measurement interval gradually was increased to a week and subsequently more for the whole experiment period of 61 weeks. During exposure of the electrode array probe in the ocean seawaters, all 100 electrodes were electrically coupled together to simulate a continuous pipe surface under marine corrosion. To measure local currents over the electrode array surface, electrode terminals of the electrode array were connected to a custom-designed multiplexer enabling the measurement of current flowing into or out of each electrode in the electrode array. A zero resistance ammeter (ZRA) was used to measure the local current flowing to (or from) any electrode in the array by connecting the ZRA between the selected electrode and the remaining 99 electrodes (switching once every 10 s). The WBE current maps were obtained by mapping local currents over the WBE every 10 min, in the same way as that described previously in references^{18–20}. Subsequently, current values were

used to plot current maps (such as those in Fig. 1a). Accumulated corrosion losses (in mm, as shown in Fig. 1c4) are calculated by accumulating metal losses that occurred over various exposure periods using Faraday's law based on a standard procedure described earlier^{18–20}.

DATA AVAILABILITY

Data sets generated during the current study are available from the corresponding author upon reasonable request.

CODE AVAILABILITY

Not applicable.

Received: 22 March 2023; Accepted: 5 August 2023;
Published online: 12 August 2023

REFERENCES

1. Evans, U.R. *The Corrosion and Oxidation of Metals: Scientific Principles and Practical Applications*. (Edward Arnold (Publishers) Ltd., 1960).
2. Melchers, R. E. A review of trends for corrosion loss and pit depth in longer-term exposures. *Corros. Mater. Degrad.* **1**, 42–58 (2018).
3. Melchers, R. E. Long-term immersion corrosion of steels in seawaters with elevated nutrient concentration. *Corros. Sci.* **81**, 110–116 (2014).
4. Melchers, R.E. Predicting long-term corrosion of metal alloys in physical infrastructure. *npj Mater. Degrad.* **3**, 4 (2019).
5. Daneshian, B., Höche, D., Knudsen, O. Ø. & Skilbred, A. W. B. Effect of climatic parameters on marine atmospheric corrosion: correlation analysis of on-site sensors data. *npj Mater. Degrad.* **7**, 1–10 (2023).
6. Melchers, R. E. & Jeffrey, R. Corrosion of long vertical steel strips in the marine tidal zone and implications for ALWC. *Corros. Sci.* **65**, 26–36 (2012).
7. Jeffrey, R. & Melchers, R. E. Corrosion of vertical mild steel strips in seawater. *Corros. Sci.* **51**, 2291–2297 (2009).
8. Melchers, R. E. Modeling of marine immersion corrosion for mild and low-alloy steels part 1: phenomenological model. *Corrosion* **59**, 319–334 (2003).
9. Melchers, R. E. & Jeffrey, R. The transition from short-to long-term marine corrosion of carbon steels: 1. Experimental observations. *Corrosion* **78**, 415–426 (2022).
10. Melchers, R. E. Recent progress in the modeling of corrosion of structural steel immersed in seawaters. *J. Infrastruct. Syst.* **12**, 154–162 (2006).
11. Paik, J.K. & Melchers, R.E. *Condition Assessment of Aged Structures*. (Elsevier, 2014).
12. Booth, F. A note on the theory of surface diffusion reactions. *Trans. Faraday Soc.* **44**, 796–801 (1948).
13. Tammann, G. *Lehrbuch Der Metallographie: Chemie Und Physik Der Metalle Und Ihrer Legierungen*. (Voss, 1923).
14. Melchers, R. E. & Wells, T. Models for the anaerobic phases of marine immersion corrosion. *Corros. Sci.* **48**, 1791–1811 (2006).
15. Melchers, R. E. Mathematical modelling of the diffusion controlled phase in marine immersion corrosion of mild steel. *Corros. Sci.* **45**, 923–940 (2003).
16. Budiansky, N. D., Bocher, F., Cong, H., Hurley, M. & Scully, J. R. Use of coupled multi-electrode arrays to advance the understanding of selected corrosion phenomena. *Corrosion* **63**, 537–554 (2006).
17. Frankel, G. & Sridhar, N. Understanding localized corrosion. *Mater. Today* **11**, 38–44 (2008).
18. Laleh, M., Xu, Y. & Tan, M. Y. A three-dimensional electrode array probe designed for visualising complex and dynamically changing internal pipeline corrosion. *Corros. Sci.* **211**, 110924 (2023).
19. Tan, M.Y. *Localised Corrosion in Complex Environments* (John Wiley & Sons, 2023).
20. Wang, M., Tan, M.Y., Zhu, Y., Huang, Y. & Xu, Y. Probing top-of-the-line corrosion using coupled multi-electrode array in conjunction with local electrochemical measurement. *npj Mater. Degrad.* **7**, 16 (2023).
21. Combrade, P. In *Corrosion Mechanisms in Theory and Practice*. 449–498 (CRC Press, 2011).
22. Herro, H.M. & Port, R.D. *The Nalco Guide to Cooling Water System Failure Analysis*. (McGraw-Hill, 1993).
23. Chaves, I. A., Melchers, R. E., Sterjovski, Z. & Rosen, J. Long-term marine immersion corrosion of welded ABS grade steels. *Corros. Eng. Sci. Technol.* **57**, 195–203 (2022).
24. Chaves, I. A. & Melchers, R. E. Pitting corrosion in pipeline steel weld zones. *Corros. Sci.* **53**, 4026–4032 (2011).

25. Southwell, C., Bultman, J. & Alexander, A. Corrosion of metals in tropical environments. Final report of 16-year exposures. *Mater. Perform.* **15**, 9–25 (1976).

ACKNOWLEDGEMENTS

Financial support from the National Decommissioning Research Initiative of National Energy Resources Australia (NREA) and Australian Research Council (ARC) Discovery project ID: DP200100568 is gratefully acknowledged. Professor John Donald, Dr Andrew Oxley, Mr James Redmond and the team in Life & Environmental Sciences, Deakin University for supporting and assisting Queenscliff field testing for acquiring localised corrosion data.

AUTHOR CONTRIBUTIONS

M.L.: methodology; experiments; validation; investigation; writing and revising. Y.H.: experiments, validation; investigation. R.E.M.: conceptualisation; validation; reviewing and editing. M.Y.J.T.: conceptualisation; methodology; writing and revising, reviewing and editing.

COMPETING INTERESTS

The authors declare no competing interests.

ADDITIONAL INFORMATION

Correspondence and requests for materials should be addressed to Mike Yongjun Tan.

Reprints and permission information is available at <http://www.nature.com/reprints>

Publisher's note Springer Nature remains neutral with regard to jurisdictional claims in published maps and institutional affiliations.



Open Access This article is licensed under a Creative Commons Attribution 4.0 International License, which permits use, sharing, adaptation, distribution and reproduction in any medium or format, as long as you give appropriate credit to the original author(s) and the source, provide a link to the Creative Commons license, and indicate if changes were made. The images or other third party material in this article are included in the article's Creative Commons license, unless indicated otherwise in a credit line to the material. If material is not included in the article's Creative Commons license and your intended use is not permitted by statutory regulation or exceeds the permitted use, you will need to obtain permission directly from the copyright holder. To view a copy of this license, visit <http://creativecommons.org/licenses/by/4.0/>.

© The Author(s) 2023